# NJC

Accepted Manuscript


This is an *Accepted Manuscript*, which has been through the Royal Society of Chemistry peer review process and has been accepted for publication.

*Accepted Manuscripts* are published online shortly after acceptance, before technical editing, formatting and proof reading. Using this free service, authors can make their results available to the community, in citable form, before we publish the edited article. We will replace this *Accepted Manuscript* with the edited and formatted *Advance Article* as soon as it is available.

You can find more information about *Accepted Manuscripts* in the Information for Authors.

Please note that technical editing may introduce minor changes to the text and/or graphics, which may alter content. The journal's standard Terms & Conditions and the Ethical guidelines still apply. In no event shall the Royal Society of Chemistry be held responsible for any errors or omissions in this *Accepted Manuscript* or any consequences arising from the use of any information it contains.

ROYAL SOCIETY OF CHEMISTRY

www.rsc.org/njc

Cite this: DOI: 10.1039/c0xx00000x

www.rsc.org/xxxxxx

PAPER

# Superior Peroxidase Memitic Activity of Carbon dots/Pt Nanocomposites Rely on Synergistic Effects

**Yuming Dong*, Jingjing Zhang, Pingping Jiang, Guangli Wang, Xiuming Wu, Hui Zhao, Chi Zhang**

***Received (in XXX, XXX) Xth XXXXXXXXX 20XX, Accepted Xth XXXXXXXXX 20XX***

**DOI: 10.1039/b000000x**

**Abstract:** Composite structures based on synergistic effect are perfect candidates to explore efficient functional materials. So far, metal/carbon dots composites have not been used as peroxidase mimetics. Herein, we reported a carbon dots/Pt nanocomposite which was synthesized by a simple method. Due to the synergistic effects between carbon dots (CDs) and Pt, the catalytic efficiency of composite was nine times and five times higher than that of carbon dots and Pt respectively. The production of active oxygen species ( OH) by $H_2O_2$ decomposition were responsible for the oxidation of TMB. On this basis, the CDs-Pt NPs were used successfully for visual and colorimetric detection of $H_2O_2$ and glucose. The detection of $H_2O_2$ and glucose are in linear range from $2.5\times10^{-6}$ to $1\times10^{-3}$ mol/L and $5\times10^{-6}$ to $5\times10^{-3}$ mol/L, with the detection limit down to 8 ×10-7 mol/L $H_2O_2$ and $1.67\times10^{-6}$ mol/L glucose respectively.

## 1. Introduction

Since magnetic iron oxide was found to exhibit an intrinsic enzyme mimetic activity similar to natural peroxidase [1], increasing attention has been paid to nanoscale peroxidase mimetics. These include $CeO_2$ [2], $V_2O_5$ nanowires [3], noble-metal nanoparticles [4-6] and carbon-based nanomaterials [7-10]. Nanomaterials as enzyme mimetic are stable, low cost, easy preparation and storage, and can be resistant to high concentrations of the substrate. The research in this field is greatly significant for new methods of analytical chemistry and biosensor. A number of nanoparticles have demonstrated their great prospects in analytical and environmental applications as enzyme mimetics [11-13]. Despite these intensive achievements, up to now, the catalytic performance of artificial enzyme still need to improve, and the research on mechanism is insufficient. Therefore, it is still a challenging task to develop efficient nano-sized enzyme memitics and further understand their catalytic mechanism.

To improve the performance, composite materials have been widely used in many fields [14-17] For instance, Pd/Pt bimetallic nanocrystals were proposed as oxygen reduction catalyst [16] and Au-$Fe_3O_4$ was used as dual imaging probes for magnetic resonance imaging and optical imaging [17]. Hence, the study of composite materials is an effective mean to explore robust functional materials. As to enzyme mimetics, the reported composite materials are mostly bimetallic alloy, metal and metal oxides composites [18-21]. Carbon dots (CDs) were firstly reported in 2004[22], and have subsequently attracted considerable attention because of their promising advantages. CDs revealed unique properties including low toxicity and molecular weight, tunable luminescence emission and high stability [23,24]. Recently, several groups have reported CDs/metal composites to improve its catalytic activity. Qi et al. suggested that carbon dots/Au exhibited excellent conductivity, stability and biocompatibility on the surface of electrode [25]. Liu et al. reported that metal nanoparticle (Ag, Au, Cu)/carbon quantum dot composite as a photocatalyst for high-efficiency cyclohexane oxidation [26]. At the same time, to the best of our knowledge, metal/carbon dots composites have not been used as peroxidase mimetics.

In light of these facts, though both CDs [27] and Pt nanoparticles [28,29] have been proposed to act as a potential peroxidase mimic respectively, the design and preparation of Pt-CDs composite are highly desirable for novel peroxidase mimic. In this study, we presented a simple approach to synthesize Pt modified CDs nanocomposite and investigated the peroxidase-like activities. The activity as peroxidase mimic was evaluated using a typical substrate 3,3′,5,5′- tetramethylbenzidine (TMB) in the presence of $H_2O_2$. Due to the synergistic effects between CDs and Pt, the catalytic efficiency of composite was nine times and five times higher than that of carbon dots and Pt respectively. The production of active oxygen species ( OH) by $H_2O_2$ decomposition were responsible for the oxidation of TMB. On this basis, the CDs-Pt NPs were used successfully for visual and colorimetric detection of $H_2O_2$ and glucose.

## 2. Experimental section

### 2.1. Chemicals and methods

Glucose oxidase (GOx) was purchased from Sigma-Aldrich. L-ascorbic acid, 3,3′,5,5′-tetramethylbenzidine (TMB) and chloroplatinic acid were purcased from Shanghai Reagent Co.(China). Phosphate buffer solution (PBS, pH 7.0) was prepared with 0.2 M $NaH_2PO_4$-$Na_2HPO_4$. Acetate buffer solution (pH 2.0 or 4.0) was 0.2 M HAc-NaAc aqueous solution. All other

chemicals were of analytical grade or better quality. Ultrapure water (Millipore, ≥18 M) was used throughout. Transmission electron microscopy (TEM) was collected on a JEM-2100 (JEOL, Japan) transmission electron microscope at an accelerating voltage of 200 kV. Energy-dispersive X-ray spectroscopy (EDX) was taken on the TEM. UV-vis absorption spectra were recorded on a TU-1901 spectrophotometer (Beijing Purkinje General, China). Fluorescence intensity was detected by a Cary Eclipse Series fluorescence spectrophotometer (Varian, American). Electrochemical experiments were conducted on a CHI800C electrochemical workstation (ChenHua, ShangHai). A three-electrode cell configuration with a catalyst modified indium tin oxide (ITO) conductive glass as the working electrode, a platinum wire as the auxiliary electrode and a saturated Ag/AgCl electrode as the reference electrode. 100 μL of catalyst aqueous solution was dropped on the conducted glass, and then the glasses were dried at 80 ℃ in air. The concentrations of the catalysts were 0.045 mg/mL, 0.00375 mg/ml and 0.040 mg/ml for CDs-Pt, CDs and Pt

### 2.2. Synthesis of Nanocomposites

The carbon dots (CDs) were synthesized by a simple hydrothermal process reported by Zhang Bing et al. [30]. In brief, L-ascorbic acid (1.1 g) was dissolved in deionized water (25 mL), and then ethanol (25 mL) was added into the solution to form a homogeneous solution under magnetic stirring. Then, an aliquot (25 mL) of the mixture was transferred into a 40 mL Teflon-lined stainless steel autoclave, heated at 180 ℃ for 4 h and then cooled to room temperature naturally. A dark brown solution was obtained, which implied the formation of the CDs. After extraction with dichloromethane, the water-phase solution was dialyzed by using cellulose ester dialysis membranes (MW: 8000-14000) for two days to remove all impurity molecules. Finally, a yellow aqueous solution containing CDs was obtained. 1 mL of 17 mM $H_2PtCl_6$ and 0.055 g $NaBH_4$ were added into 50 mL of 0.00375 mg/ml CDs aqueous solution under magnetic stirring for 48 h. The resulting product was named CDs-Pt. Pt nanoparticles (NPs) were synthesized in the similar way except replacing carbon dots solution with pure water.

### 2.3. Hydroxyl radical confirmation

50 mM $H_2O_2$, $2.5\times10^{-4}$ M terephthalic acid and different concentrations of CDs-Pt reacted in 50 mM HAc-NaAc buffer (pH 4.0) at 20 ℃ for 5 min. The solutions were used for fluorometic measurement.

### 2.4. $H_2O_2$ detection using CDs-Pt as peroxidase mimetics

A typical colorimetric analysis was realized as follows. 1 mL of 1 mM TMB, 100 μL of 1.8 mg $mL^{-1}$ CDs-Pt, and 100 μL of $H_2O_2$ (with different concentrations) were added into 2.8 mL of 200 mM acetate buffer (pH 4.0) at 20 ℃. And the mixed solution was used for adsorption spectroscopy measurement.

### 2.5. Glucose detection using GOx and CDs-Pt

Glucose detection was realized as follows: (1) 10 μL of 5.0 mg $mL^{-1}$ GOx and 100 μL of glucose with different concentrations in 0.2 M phosphate buffered saline (PBS, pH 7.0) were incubated at 37 °C for 30 min; (2) 200 μL of 5 mM TMB, 700 μL of 0.17 mg $mL^{-1}$ CDs-Pt, and 1 mL of 0.2 M acetate buffer (pH 4.0) were added into the above glucose reaction; (3) the mixed solution was incubated at 20 ℃ for 10 min and analyzed at 652 nm to determine TMB conversion.

## 3. Result and discussion

### 3.1. Characterization of the CDs-Pt composites

TEM (Fig.S1A) revealed that the particle size of CDs was about 5~6 nm, and CDs were evenly dispersed. As shown in Fig.S1B, the particle size of CDs-Pt was about 10 nm. The red circle position in Fig.S1B of CDs-Pt was detected by energy-dispersive X-ray (EDX) spectrum as shown in Fig.S1C. It was observed that the nanoparticles were composed of C and Pt, and contained 43% carbon. Fig.S1D showed the TG curve of CDs-Pt under oxygen atmosphere, the quality of the sample decreased about 40% at 800°C due to the loss of carbon, this was consistent with the results of EDX. Fig.S2 showed UV-vis absorption spectra of CDs, Pt and CDs-Pt respectively. Pt had no absorption peak in the wavelength range of 200-800 nm. Compared with CDs, the peak intensity of CDs-Pt at 262 nm dropped about 50%, indicating the formation of CDs-Pt via the combination between CDs and Pt. In Fig.S3, a strong fluorescence emission spectrum of CDs centered at 450 nm was observed when it was excited at 359 nm, while the emission intensities of both CDs-Pt and Pt at 450 nm were very weak. Fluorescence intensity of CDs was 19 times larger than that of CDs-Pt, indicating the existence of electron transfer in the CDs-Pt. It also proved the generation of CDs-Pt.

### 3.2. Peroxidase-like activities and steady-state kineticassay of the CDs-Pt composites

To investigate the peroxidase-like activity of CDs-Pt, the catalysis oxidation of peroxidase substrate 3,3′,5,5′-tetramethylbenzidine(TMB) was studied in the presence of $H_2O_2$. As shown in Fig.1, CDs-Pt can catalyze the oxidation of TMB by $H_2O_2$ which produce typical blue color with a maximum absorbance at 652 nm. The catalytic activity of CDs-Pt was nine times, five times and four times higher than that of carbon dots, Pt, and the physical mixture of CDs and Pt, respectively. This indicates the obvious synergistic effect between the two compositions rather than the physical combination.

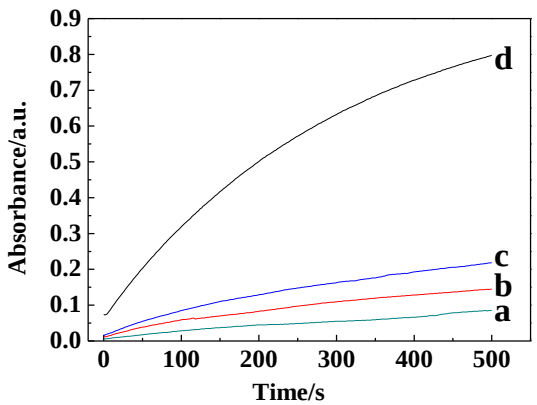


**Fig.1.** Time-dependent absorbance changes of TMB at 652 nm in different reaction systems: (a) CDs+TMB+$H_2O_2$, (b) Pt+TMB+$H_2O_2$, (c) CDs+Pt+TMB+$H_2O_2$, (d) CDs-Pt+TMB+$H_2O_2$. Reaction conditions: 0.25 mM TMB, [CDs-Pt] =0.045 mg/mL, [CDs] =0.00375 mg/ml, [Pt] =0.04 mg/ml, 50 mM $H_2O_2$ in 50 mM HAc-NaAc buffer (pH 4.0).

The ratio of components in composite material would have a

certain influence on catalytic performance. We varied the molar ratio of $H_2PtCl_6$ and CDs from 0 to 6 to study the composition dependence of the catalytic activity of CDs-Pt (Fig.2). The results demonstrated that CDs-Pt exhibited the best catalytic activity when the Pt/C molar ratio was equal to 2. When the amount of CDs was more, lots of CDs were not linked with Pt, resulting in poor performance. At the same time, Pt existed in the element form when CDs were little, and CDs were not combining with the valid active sites of Pt. The results also demonstrated that CDs-Pt composite material exhibit superior synergistic effect between CDs and Pt, especially Pt/C was equal to 2.

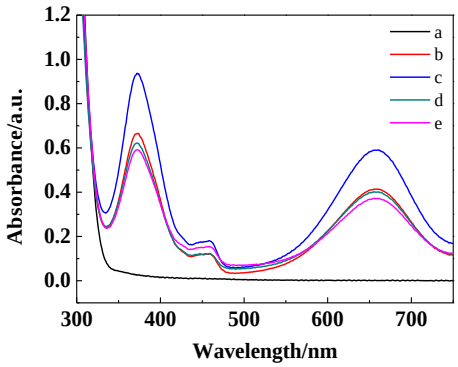


**Fig.2.** UV-vis spectra of TMB solutions in presence of $H_2O_2$ and synthetic material with different $H_2PtCl_6$/CDs molar ratio. (a) 0:1, (b) 1:1, (c) 2:1, (d) 4:1, (e) 6:1. Reaction conditions: 0.25 mM TMB, 50 mM $H_2O_2$ in 50 mM HAc-NaAc buffer (pH4.0) for 10 min.

Similar to HRP [31], the catalytic activity of CDs-Pt is dependent on pH, concentration of catalyst and $H_2O_2$ concentration. We measured the peroxidase-like activity of the CDs-Pt by varying the pH from 2.0 to 8.0, the catalyst concentration from 0.01 to 0.09 mg/mL (Fig.S4) and the $H_2O_2$ concentration from 10 mM to 100 mM (Fig.S5). Under acidic conditions, the absorbance was larger than that in neutral and basic solutions. Because proton was one of the reactants as shown in Scheme 1, the increase of $H^+$ concentration contributed to speeding up the reaction. And the optimal catalyst concentration was 0.045 mg/mL. When the catalyst concentration is larger, further oxidation of TMB could happen. As the hydrogen peroxide concentration rising, the absorbance became larger. When the $H_2O_2$ concentration was 50 mM, the absorbance reached about 1.

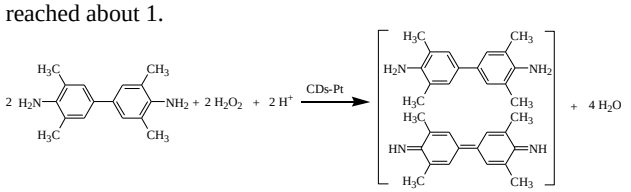


**Scheme.1.** The corresponding reaction equation of TMB oxidization by $H_2O_2$ in presence of CDs-Pt.

The apparent steady-state reaction kinetic parameters by initial rate method were determined to investigate the peroxidase-like mechanism. Apparent steady-state reaction parameters at different concentrations of substrate were obtained by calculating the slopes of initial absorption changes with time. As shown in Fig.3, the curves indicated the typical Michaelis-Menten kinetic for the oxidation of TMB by varying the concentration of TMB. The data was fitted to the Michaelis-Menten equation to determine the catalytic parameters. The $K_m$ of HRP for TMB was 4.36 times higher than that of CDs-Pt (Table.1), suggesting that CDs-Pt have a higher affinity for TMB than HRP. The maximal reaction velocity of CDs-Pt was about five times and two times larger than that of CDs [27] and Pt [29] respectively, indicating a higher peroxidase-like activity of the composites.

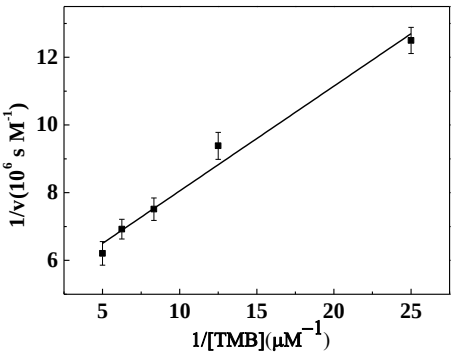


**Fig.3.** Steady-state kinetic analysis using Michaelis-Menten model for CDs-Pt by varying the concentration of TMB. Reaction conditions: [CDs-Pt] = 0.045 mg/mL, 50 mM $H_2O_2$ in 50 mM HAc-NaAc buffer (pH 4.0). Error bars represent the standard deviation for three measurements as well as the following figures.

**Table.1.** Comparison of the kinetic parameters between CDs-Pt and reported results. $K_m$ is the Michaelis-Menten constant, $V_{max}$ is the maximal reaction rate.

| | $K_m$[mM] | $V_{max}$[M $s^{-1}$] |
|---|---|---|
| HRP[7] | 0.275 | $2.46\times10^{-8}$ |
| $Fe_3O_4$[20] | 0.485 | $5.63\times10^{-8}$ |
| $Fe_3O_4$@Pt[20] | 0.147 | $7.11\times10^{-8}$ |
| CDs[27] | 0.040 | $3.61\times10^{-8}$ |
| Pt[29] | 0.0186 | $1.18\times10^{-7}$ |
| CDs-Pt | 0.063 | $2.02\times10^{-7}$ |

In the reaction which containing hydrogen peroxide, free hydroxyl radicals are usually among important intermediates. The nature of peroxidase-like activity of CDs-Pt may originate from their catalytic ability to decompose $H_2O_2$ into OH. In order to study the mechanism, terephthalic acid was adopted as a fluorescence probe to evaluate the effects of the CDs-Pt on OH intensity, because terephthalic acid easily react with OH to form highly fluorescent 2-hydroxy terephthalic acid [32].

Under the excitation light of 315 nm (Fig.S6), the CDs-Pt catalyst itself did not show fluorescence peak at 425 nm, while there was certain fluorescence intensity at 425 nm. When terephthalic acid, hydrogen peroxide and CDs-Pt were mixed, the characteristic fluorescence peak of 2-hydroxy terephthalic acid at 425 nm was observed (Fig.S7). It indicated the generation of OH radicals in presence of hydrogen peroxide and CDs-Pt. When we subtract the fluorescence intensity of CDs-Pt itself at 425 nm (Fig.S6), gradual increase of the fluorescence intensity was observed as the concentration of CDs-Pt increased (Fig.4), suggesting the increase of OH radicals. It can be concluded that CDs-Pt catalyze the decomposition of $H_2O_2$ into OH radicals under acidic conditions.

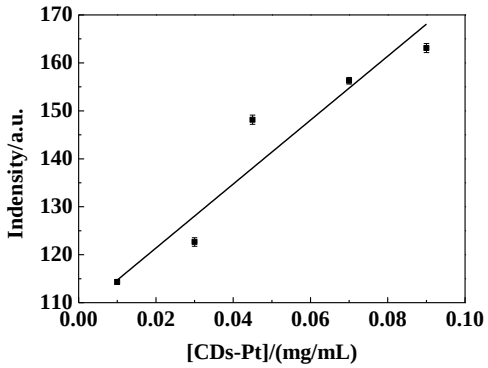


**Fig.4.** The fluorescence intensity of 2-hydroxy terephthalic acid along with CDs-Pt concentration in presence of $H_2O_2$ (after subtract fluorescence intensity of CDs-Pt at 425 nm). Reaction conditions: 50 mM $H_2O_2$, $2.5\times10^{-4}$ M terephthalic acid, in 50 mM HAc-NaAc buffer (pH 4.0) for 5 min.

In order to further prove the role of OH, the TMB oxidation experiments were carried out in the presence of a free radical scavenger *tert*-butanol, which can quickly react with OH, and terminate radical chain reactions by generating inert intermediates radicals[33]. As shown in Fig.5, with the increasing tert-butanol concentration from 0 to 150 mg/mL, the absorbance of oxidized TMB decreased gradually. When the concentration of tert-butyl alcohol was 25 mg/mL, the absorbance dropped about 50%. This result validated that OH was the active oxygen species in TMB oxidation system with CDs-Pt.

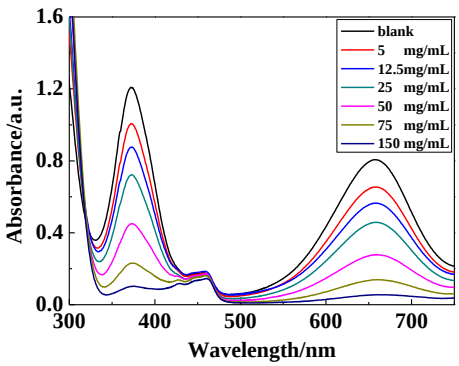


**Fig.5.** Effects of *tert*-butanol concentration on the oxidation of TMB. Reaction conditions: 0.25 mM TMB, [CDs-Pt] = 0.045 mg/mL, 50 mM $H_2O_2$ in 50 mM HAc-NaAc buffer (pH 4.0) for 10 min.

The electron transfer progress is very important for catalytic reaction system, especially oxidation-reduction reaction. Therefore, electrochemical performance of as-prepared catalyst was discussed here to explain the catalytic mechanism. The cyclic voltammetry behaviors of blank ITO, CDs, Pt and CDs-Pt modified ITO electrodes were investigated in 50 mM HAc-NaAc buffer solution in presence of 100 mM $H_2O_2$. Within the scope of the scanning potential (-0.2V to 0.3V vs Ag/AgCl), the current was negative. It suggested that the electron transferred from the electrode to the solution, and then hydrogen peroxide got electron and was reduced to hydroxyl ion. In absence of TMB, the current intensity of CDs-Pt modified electrode was the highest, which was 4 times, 3 times and 2.5 times larger than that of blank, CDs and Pt modified electrodes, respectively (Fig.6A). It can be concluded that CDs-Pt revealed the best catalytic performance in electrochemical reduction of $H_2O_2$. When TMB were added (Fig.6B), current signal of CDs-Pt modified electrode was sharply decreased to just about 10% of its original value. At the same time, only slight weakening was observed for blank, CDs and Pt modified electrodes. The obvious difference on current change (before and after TMB addition) among CDs, Pt and CDs-Pt suggested remarkable dissimilar surface activity to TMB, which is accordant with their catalytic activity (Fig.1). In the catalytic oxidation process, TMB acted as an electron donor and $H_2O_2$ was an electron acceptor. In presence of TMB, electrons transferred quickly from TMB to $H_2O_2$ on the surface of CDs-Pt, and then the electron transfer amount from the ITO electrode to the solution was depressed, leading to sharp decrease of current compared with the condition without TMB. From these results, it can be said that CDs-Pt revealed best sensitivity to both $H_2O_2$ and TMB, which was essential for its catalytic activity. The results also proved the obvious synergistic effect between CDs and Pt.

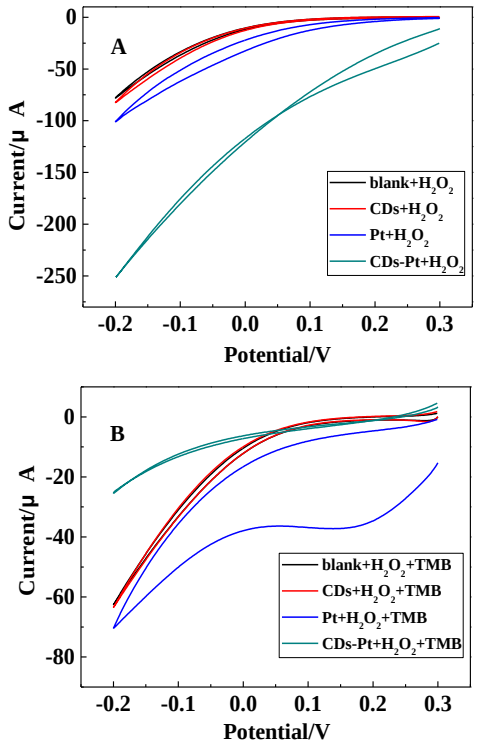


**Fig.6.** Cyclic voltammetry scans with CDs, Pt and CDs-Pt modified electrodes in 50 mM HAc-NaAc buffer (pH 4.0), the concentration of hydrogen peroxide is 100 mM. A: without TMB; B: with 0.25 mM TMB.

The accurate and rapid determination of $H_2O_2$ is of practical importance in environmental and bioanalytical fields [34]. Because the catalytic oxidation of TMB is $H_2O_2$ concentration dependent, the system could be used to detect $H_2O_2$. Under the optimal conditions, the catalytic system was used for $H_2O_2$ detection. Fig.7 showed a typical $H_2O_2$ concentration-response curve, where as low as $8\times10^{-7}$ mol/L $H_2O_2$ was detected with a linear range from $2.5\times10^{-6}$ to $1\times10^{-3}$ mol/L. According to the insert, the regression equation is $(Abs-Abs_0) = 1.220\ [H_2O_2] + 0.0066$ ($R^2$=0.9806).



 

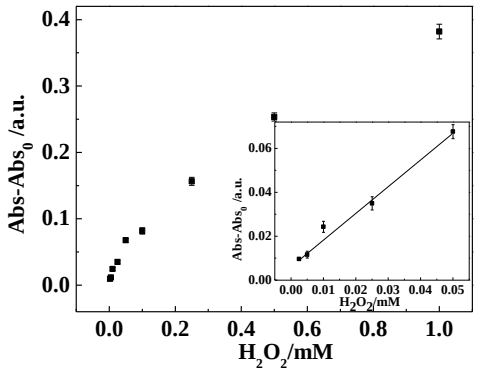


**Fig.7.** A dose-response curve for $H_2O_2$ detection using CDs-Pt as artificial enzyme ($Abs_0$: the absorbance at 652 nm without the catalyst). The insert showed the linear calibration plot for $H_2O_2$ using CDs-Pt. Reaction conditions: 0.25 mM TMB, [CDs-Pt] =0.045 mg/mL in 50 mM HAc-NaAc buffer (pH 4.0) for 10 min.

Because $H_2O_2$ is the main product of the glucose oxidase (GOx)-catalyzed reaction, combined with glucose oxidase, the proposed method could be used for the determination of glucose, which is an important indicator for the diagnosis of diabetes mellitus in clinical medicine. The linear range for glucose was determined as from $5\times10^{-6}$ to $5\times10^{-3}$ mol/L (Fig.8). The regression equation is (Abs-$Abs_0$)=0.162 log$C_{glucose}$ + 0.506 ($R^2$=0.9875).The limit of detection of this assay for glucose was $1.67\times10^{-6}$ mol/L, which is lower than obtained using Carbon nanodots and positively charged gold NPs as peroxidase mimetic[4,27].

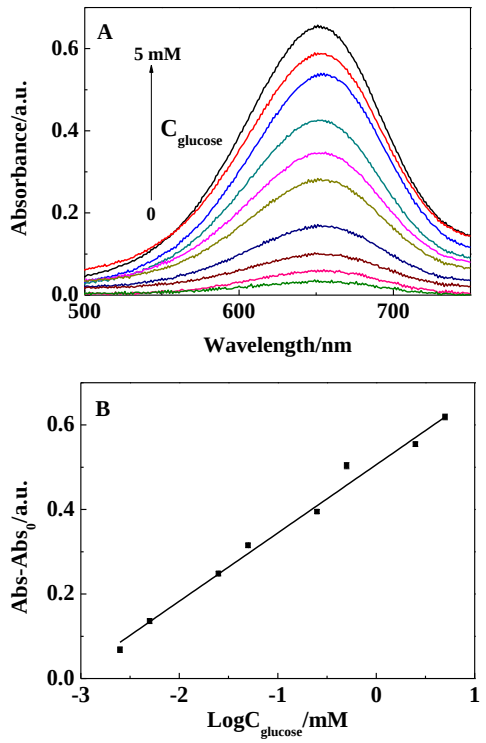


**Fig.8.** A: A dose-response curve for glucose detection using CDs-Pt ($Abs_0$: the absorbance at 652 nm without the catalyst). B: Linear relationship between the Abs-$Abs_0$ of 652 nm and glucose concentrations. Reaction conditions: 0.5 mM TMB, [GOx]=0.025 mg/mL, [CDs-Pt]=0.0595 mg/mL in 100 mM HAc-NaAc buffer (pH 4.0) for 10 min.

## 4. Conclusions

In summary, CDs-Pt nanocomposites were prepared and proposed as a robust enzyme memitic for the first time. Compared with HRP and many reported nano peroxidase mimetic, CDs-Pt revealed superior catalytic activity. Compared with carbon dots and Pt NPs, the synergistic effect between CDs and Pt was proved as the key factor for catalysis. By an electrochemical method, excellent sensitivity of CDs-Pt to both $H_2O_2$ and TMB was discovered. OH generated by $H_2O_2$ decomposition was responsible for the oxidation of TMB. Based on the efficient peroxidase-like performance, the CDs-Pt NPs were used successfully for visual and colorimetric detection of $H_2O_2$ and glucose, and the detection limit was $8\times10^{-7}$ mol/L to $H_2O_2$ and $1.67\times10^{-6}$ mol/L to glucose respectively. This work provides a novel kind of material for the field of enzyme memetics as well as other functional applications.

## Acknowledements

The authors gratefully acknowledge the support from the National Natural Science Foundation of China (No. 20903048, 21275065), the Fundamental Research Funds for the Central Universities (JUSRP51314B) and MOE & SAFEA for the 111 Project (B13025).

## Notes and references

[a] *Key Laboratory of Food Colloids and Biotechnology (Ministry of Education of China), School of Chemical and Material Engineering, Jiangnan University, Wuxi 214122, P. R. China. Fax: (+) 86-510-85917763. E-mail: dongym@jiangnan.edu.cn*

† Electronic Supplementary Information (ESI) available: The characterization results of CDs-Pt, the catalytic performance of CDs-Pt under different conditions, the fluorescence spectra of CDs-Pt and 2-hydroxy terephthalic acid can be found in Supporting Information. See DOI: 10.1039/b000000x/

[1] L. Z. Gao, J. Zhuang, L. Nie, J. B. Zhang, Y. Zhang, N. Gu, T. H. Wang, J. Feng, D. L. Yang, S. Perrett and X. Y. Yan, *Nat. Nanotechnol*., 2007, **2**, 577-583.
[2] X. Jiao, H. J. Song, H. H. Zhao, W. Bai, L. C. Zhang and Y. Lv, *Anal. Methods*., 2012, **4**, 3261-3267.
[3] R. Andr é, F. Nat álio, M. Humanes, J. Leppin, K. Heinze, R. Wever, H. C. Schr öder and W. E. G. M üller, *Adv. Funct. Mater*., 2011, **21**, 501-509.
[4] Y. Jv, B. X. Li and R. Cao, *Chem. Commun.*, 2010, **46**, 8017-8019.
[5] H. Jiang, Z. H. Chen, H. Y. Cao and Y. M. Huang, *Analyst*, 2012, **137**, 5560-5564.
[6] J. B. Liu, X. N. Hu, S. Hou, T. Wen, W. Q. Liu, X. Zhu and X. C. Wu, *Chem. Commun*., 2011, **47**, 10981-10983.
[7] X. C. Wu, Y, Zhang, T. Han, H. X. Wu, S. W. Guo and Ji. Y. Zhang, *RSC Adv*., 2014, **4**, 3299-3305.
[8] M. Liu, H. M. Zhao, S. Chen, H. T. Yu and X. Quan, *Chem. Commun*., 2012, **48**, 7055-7057.
[9] R. J. Cui, Z. D. Han and J. J. Zhu, *Chem. Eur. J.*, 2011, **17**, 9377-9384.
[10] S. Liu, J. Q. Tian, L. Wang, Y. L. Luo and X. P. Sun, *RSC Adv.*, 2012, **2**, 411-413.
[11] C. O. Song, J. W. Lee, H. S. Choi and J. K. Kang, *RSC Adv.*, 2013, **3**, 20179-20185.
[12] C. W. Lien, C. C. Huang and H. T. Chang, *Chem. Commun*., 2012, **48**, 7952-7954.
[13] W. Wang, X. P. Jiang and K. Z. Chen, *Chem. Commun.*, 2012, **48**, 7289-7291.

[14] K. Jia, M. Y. Khaywah, Y. G. Li, J. L. Bijeon, P. M. Adam, R. Deturche, B. Guelorget, M. Francois, G. Louarn and R. E. Ionescu, *ACS Appl. Mater. Interfaces*., 2014, **6**, 219-227.
[15] Y. He and H. Cui, *J. Phys. Chem. C*, 2012, **116**, 12953-12957.
[16] B. Lim, M. Jiang, P. H. C. Camargo, E. C. Cho, J. Tao, X. Lu, Y. Zhu and Y. N. Xia, *Science* 2009, **324**, 1302-1305.
[17] H. Yu, M. Chen, P. M. Rice, S. X. Wang, R. L. White and S. H. Sun, *Nano Lett.*, 2005, **5**, 379-382.
[18] C. W. Tseng, H. Y. Chang, J. Y. Chang and C. C. Huang, *Nanoscale*, 2012, **4**, 6823-6830.
[19] H. Y. Chen, Y. Li, F. B. Zhang, G. L. Zhang and X. B. Fan, *J. Mater. Chem.*, 2011, **21**, 17658-17661.
[20] M. Ma, J. Xie, Y. Zhang, Z. P. Chen and N. Gu, *Mater. Lett.*, 2013, **105**, 36-39.
[21] J. Liu, W. Zhang, H. L. Zhang, Z. Y. Yang, T. R. Li, B. D. Wang, X. Huo, R. Wang and H. T. Chen, *Chem. Commun.*, 2013, **49**, 4938-4940.
[22] X. Y. Xu, R. Ray, Y. L. Gu, H. J. Ploehn, L. Gearheart, K. Raker and W. A. Scrivens, *J. Am. Chem. Soc.*, 2004, **126** (40), 12736-12737.
[23] S. C. Ray, A. Saha, N. R. Jana and R. Sarkar, *J. Phys. Chem. C*, 2009, **113**, 18546-18551.
[24] S. N. Baker and G. A. Baker, *Angew. Chem. Int. Ed.*, 2010, **49**, 6726-6744.
[25] Q. Gao, J. M. Han and Z. F. Ma, *Biosens. Bioelectron.*, 2013, **49**, 323-328.
[26] R. H. Liu, H. Huang, H. T. Li, Y. Liu, J. Zhong, Y. Y. Li, S. Zhang and Z. H. Kang, *ACS Catal.*, 2014, **4**, 328-336.
[27] W. B. Shi, Q. L. Wang, Y. L. Long, Z. L. Cheng, S. H. Chen, H. Z. Zheng and Y. M. Huang, *Chem. Commun.*, 2011, **47**, 6695-6697.
[28] M. Ma, Y. Zhang and Gu. N. *Colloids and Surfaces A: Physicochem. Eng. Aspects*, 2011, **373**, 6-10.
[29] K. Cai, Z. C. Lv, K. Chen, L. Huang, J. Wang, F. Shao, Y. J. Wang and H. Y. Han, *Chem. Commun.*, 2013, **49**, 6024-6026.
[30] B. Zhang, C. Y. Liu and Y. Liu, *Eur. J. Inorg. Chem*., 2010, **28**, 4411-4414.
[31] K. Chattopadhyay and S. Mazumdar, *Biochemistry*, 2000, **39**, 263-270.
[32] K. Ishibashi, A. Fujishima, T. Watanabe and K. Hashimoto, *Photochem. Photobiol. A*, 2000, **134**, 139-142.
[33] G. V. Buxton, C. L. Greenstock, W. P. Heiman and A. B. Ross, *J. Phys. Chem.* Ref. Data., 1988, **17**(2). 513-886.
[34 O. S. Wolfbeis, A. DÜrkop, M. Wu and Z. H. Lin, *Angew. Chem. Int. Ed.*, 2002, **41**, 4495-4498.



 